

# Factors affecting the performance of the bimorph-based dilatometer for field induced strain measurement of polymer films

Shishang Guo<sup>a)</sup>

*Department of Applied Physics, the Hong Kong Polytechnic University, Hung Hom, Kowloon, Hong Kong, People's Republic of China and Department of Physics, Wuhan University, Wuhan 430072, People's Republic of China*

H. L. W. Chan

*Department of Applied Physics, the Hong Kong Polytechnic University, Hung Hom, Kowloon, Hong Kong, People's Republic of China*

X.-Z. Zhao

*Department of Physics, Wuhan University, Wuhan 430072, People's Republic of China*

C. L. Choy

*Department of Applied Physics, the Hong Kong Polytechnic University, Hung Hom, Kowloon, Hong Kong, People's Republic of China*

(Received 5 August 2002; accepted 2 December 2002)

This article gives a detailed discussion about the design and performance of a bimorph-based dilatometer using different sensor heads and platforms both experimentally and theoretically. A current preamplifier in high-pass filter mode was used to optimize the signal and a protective circuit was introduced. The test results demonstrated that the best signal occurred when the lengths of stainless steel pin and bimorph were both 10.0 mm and that the resonant frequency was inversely proportional to the square of the sensor length. Some suggestions for reducing the noise and improving the sensitivity were also provided. © 2003 American Institute of Physics.

[DOI: 10.1063/1.1539897]

## I. INTRODUCTION

Several years ago, it was found that poly(vinylidene fluoride-trifluoroethylene) [P(VDF-TrFE)] copolymer has a large longitudinal electrostrictive strain (more than 4.5%) after proper electron irradiation.<sup>1,2</sup> A bimorph-based dilatometer was then designed to characterize the electric field induced strain response in the vertical direction, parallel to the electric field, in thin and soft free standing polymer films over a relatively wide frequency range (0.1 Hz–1 kHz).<sup>3,4</sup> The results showed that it is capable of detecting displacement down to subangstrom range with high sensitivity. Many works have been done to improve the stability and reliability of this dilatometer, and it is believed to be the best way to measure the field induced strain in thin and soft polymer films under high voltage at low frequencies so far.<sup>4,5</sup>

Compared with other methods for strain measurement, the sensitivity of the bimorph-based sensitivity is strongly dependent on the design and installation of the bimorph and its appendix.<sup>6,7</sup> Careful preparation of bimorph, including sputtering electrodes, adhering with appropriate epoxy and assembling in a housing plays a key role. Variation of the length of the stainless steel pin can also cause a notable change of output signal produced by the bimorph.

However, the bimorph-based dilatometer can avoid sever errors existing in those conventional methods for its unique design to measure thin and soft free standing polymer films.

Figure 1 is a schematic demonstration of the setup. Under an external electric field, the polymer film sample expands and contracts in the  $z$  direction and generates a corresponding motion in the sensor head. Consequently, a bending in the piezoelectric bimorph is produced and through the direct piezoelectric effect an electrical output, which is proportional to the sensor head displacement, is generated. After calibration, this output signal can be used to quantitatively measure the strain of the sample.<sup>3</sup>

In this article, we will first discuss the different bimorph

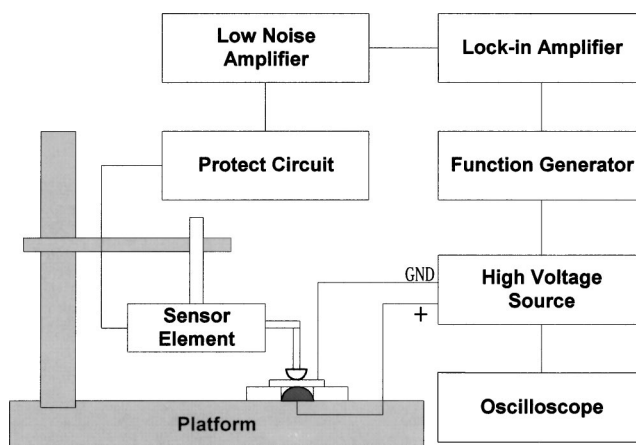


FIG. 1. Schematic demonstration of the bimorph-based dilatometer. The lock-in amplifier in current mode has sensitivity down to the  $fA$  range and the time constant is 30 s for signals at 1 Hz and 1 s at 1 kHz.

<sup>a)</sup>Author to whom correspondence should be addressed; electronic mail: apssguo@polyu.edu.hk

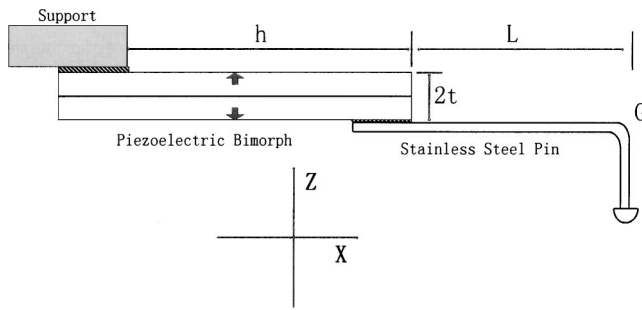


FIG. 2. Schematic demonstration of the sensor head. The displacement of the stainless steel pin at the point  $G$  causes the bending of the bimorph to generate a proportional current output.

sensor head designs and their calibrated performance, and then the whole setup is analyzed both from electrical and mechanical viewpoints. Some suggestions are also provided according to the experiment conditions for further improving the reliability of this instrument.

## II. EXPERIMENT

We fabricated different sensor heads in order to obtain the optimum relationship between the length of bimorph and the stainless steel pin. The schematic demonstration is shown in Fig. 2. The bimorphs were commercial products and their dimensions are: thickness  $t=0.51$  mm, width  $w=1.48$  mm, and whole length  $h=15.02$  mm. The upper and lower surfaces of bimorph were sputtered with chromium buffer layer (typically 100–200 Å thick) and gold outer layer (typically 400–600 Å thick) as electrodes. After the connection of the bimorph and stainless steel pin, the whole head was attached to a brass stage specially designed for this setup by epoxy glue at the signal port of the bimorph. Among these sensor heads, five types were chosen to analyze as listed in Table I.

No. 1 and No. 2 were similar as a reference. The  $h$  and  $L$  of them varied because they were the most important factors in this setup. In order to estimate which one was the best for measurement, a standard piezoelectric ceramic pad sample of Model ZJ-3B Piezo d33 Meter, whose  $d_{33}=301$  pC/N, was employed as calibration standard. First the standard sample was used to get a group of data as a base line for a calibration curve of different sensor heads, and then the  $d_{33}$  of other samples was induced. From the measured values obtained by

TABLE I. Different sensor heads and their calibration.

| Sensor heads          | S.S. pin (mm) <sup>a</sup> | Bimorph (mm) | PZT-5 (491 pC/N) <sup>c</sup> | PMN/PT (460 pC/N) <sup>d</sup> |
|-----------------------|----------------------------|--------------|-------------------------------|--------------------------------|
| No. 1(2) <sup>b</sup> | 13.5(13)                   | 13.5(13)     | 396                           | 298                            |
| No. 3                 | 10                         | 10           | 509                           | 464                            |
| No. 4                 | 5                          | 10           | 562                           | 564                            |
| No. 5                 | 0                          | 10           | 761                           | 675                            |

<sup>a</sup>S. S. pin is the abbreviation of stainless steel pin.

<sup>b</sup>No. 1 and No. 2 are similar with a slight difference in the length as reference.

<sup>c</sup>PZT-5 is made from PKI-552 commercial powders; 491 pC/N is the measured value, thickness is 1.54 mm and diameter is 13.57 mm.

<sup>d</sup>PMN/PT pad is in the ratio of 65%/35%, sintered at 1200 °C and poled under 3 kV/m; 460 pC/N is the measured values and thickness is 0.86 mm and diameter is 10.47 mm.

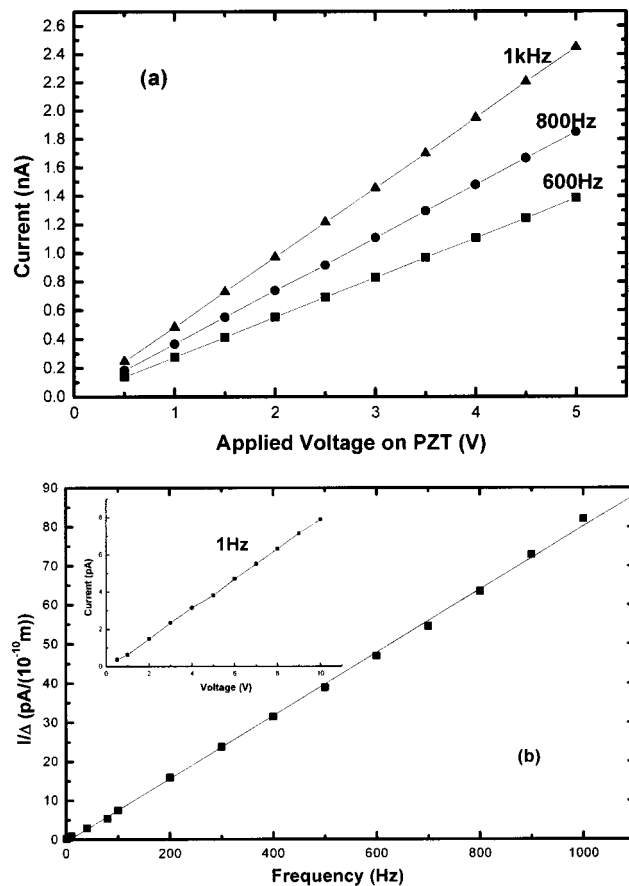


FIG. 3. (1) The current measured by a lock-in amplifier at different frequencies vs displacement in a PZT standard (the displacement in PZT= $4.91 \text{ \AA} \times$  Applied Voltage) cure. (b) The calibration curve of the bimorph sensor. The inserted graph is the calibration curve of 1 Hz with 30 s time constant of the lock-in amplifier. Open circles are the experimental data and solid line is a linear fitting curve.

Model ZJ-3B Piezo d33 Meter, it can be seen that the values obtained by No. 3 head were closest to the correct values as shown in Table I. Figure 3 is the calibration curve of the No. 3 head at different frequencies. In our experiment system, the PZT-5 listed in Table I was chosen as the calibration standard because of its biggest piezoelectric constant  $d_{33}$  (491 pC/N) and No. 3 was used as an appropriate sensor head in the following measurements.

Two platforms for different samples under different applied electric fields were designed as presented in Fig. 4. Figure 4(a) was one suitable for many kinds of piezoelectric materials like ceramic pads and polymer films under low electric field. This platform had a Teflon container to load sample. Thin conducting electrode (chromium/gold) was evaporated on a glass substrate and then the glass substrate was pasted on the bottom container. Two special pins were installed. One was connected to the electrode as the high voltage input and the other was connected to the sample as ground. The electric field was provided by a high voltage amplifier (Trek Model 663A Power Supply and Model 662±10 kV amplifier). An oscilloscope (Hewlett-Packard 54645A Oscilloscope) was used to monitor the high voltage signal. Figure 4(b) was a platform suitable for soft and thin polymer films when a high voltage was needed. A brass con-

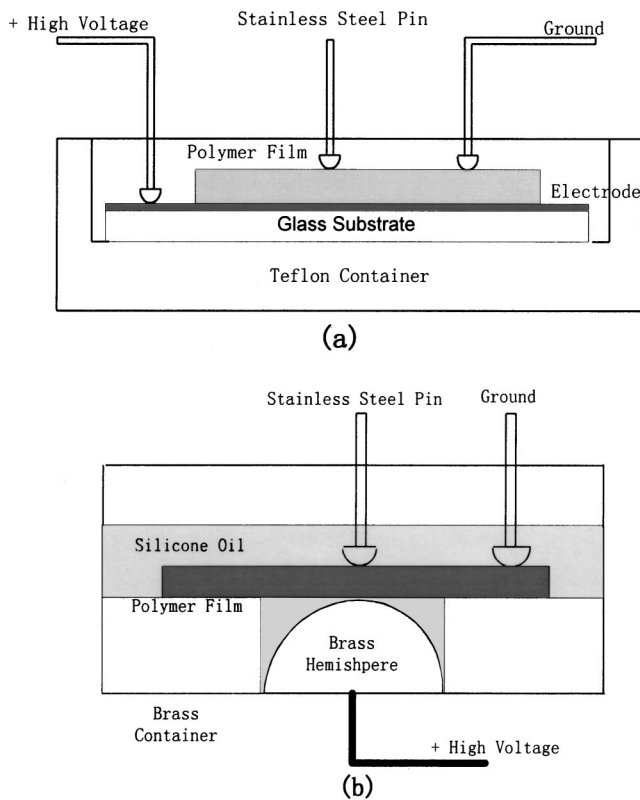


FIG. 4. (a) The platform for piezoelectric ceramic materials and polymer films under a low electric field. (b) The platform for thin and soft polymer films under a relative high electric field when samples are immersed in insulated oils (silicon oil).

tainer was machined and a brass hemisphere was buried in a Teflon holder while just exposing a point of the surface. Then the Teflon holder was attached on Bakelite pad and the high voltage was led to the brass hemisphere through a hole drilled on the center of holder. Another ground pin was installed to touch the sample as illustrated. Under high electric field the film was clamped by the stainless steel pin and the point of brass hemisphere immersed in insulated oil (silicon oil, capacitor oil, etc.) in void of spark. It will expand or contract in the longitudinal direction when driven by electric field, so the pin as ground should contact the edge of the sample solidly and cannot vibrate.

The bimorph-based dilatometer is very sensitive to low frequencies, so it is necessary to fix the bimorph housing to reduce vibration.<sup>3</sup> On the other hand, the environmental noise such as air turbulence and electromagnetic disturbance can also limit the probe sensitivity greatly. A method to reduce the noise is to put this setup in a closed chamber but it is not convenient to operate during the measurement. In our setup, a shielding housing was designed only to enclose the bimorph, and a BNC female connector was installed to lead the signal out to a lock-in amplifier (Model SR850 DSP lock-in amplifier). This part was fixed on a stage that can move along *x-y-z* directions precisely. A voltage (0.05–10 V) generated by an arbitrary function generator (Sony Tektronix AFG310) was amplified by the high voltage amplifier and then applied to the sample as high electric field. Considering the polymer film may break down under high voltage and cause severe damage to the lock-in amplifier due to the short

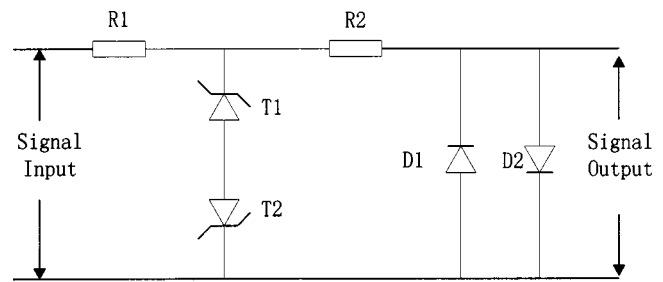


FIG. 5. The schematic of protective circuit between the output of bimorph and lock-in amplifier.

voltage pulse induced by the bimorph, we added a protective circuit in front of the current output of the bimorph as shown in Fig. 5. If the input voltage amplitude was beyond 0.6 V, the diode would short circuit and keep the signal from inputting to the lock-in amplifier. The transient voltage suppressor has a 5 V normal value. A brass box shielded the circuit to reduce the electrical noise. A very small current increase was induced by the protect circuit in series with the sensor element. It may be caused by the current leakage of the transient voltage suppressor and diode of the protective circuit. However, the current change was regular and linear, which had no effect on the results according to the experimental process.

In order to optimize the output signal, a low-noise current amplifier (Model SR570 low-noise current preamplifier) was used to transform the signal from current mode to voltage mode. The frequency filter was set at a high pass of 0.1 Hz and sensitivity of 500  $\mu\text{A/V}$  at 1 kHz. As shown in Fig. 6, no significant changes in calibration occurred in this situation. The advantage of a current preamplifier is to overcome the cable loading of the active element of bimorph; the closer to the bimorph, the lower will be the contribution of the cable to the overall noise level.<sup>8</sup>

### III. ANALYSIS OF THE PERFORMANCE

It is necessary to analyze the performance of the bimorph first and then characterize the setup under different situations. In this setup, the bimorph and stainless steel pin are treated as a cantilever system with one end clamped. From Ref. 3, the relationship between the force and the displacement  $\Delta$  at the sensor head (point *G*) is

$$\Delta = BF, \tag{1}$$

where *F* is the force imposed on the sample and *B* is a constant presented as

$$B = \frac{4L^3}{3\pi Y^{st}r^4} + \frac{3h}{2wt^3Y}(hL + L^2 + h^2/3)$$

and we also get the charge *q* and the displacement  $\Delta$  at the tip *G* of the stainless steel pin in the following equation:

$$q = -\frac{3d_{31}(h^2 + 2Lh)}{8t^2B}\Delta, \tag{2}$$

where *r* is the radius and *Y<sup>st</sup>* is the Young's modulus of the stainless steel pin, respectively. And *d<sub>31</sub>* is the piezoelectric constant and *Y* is the Young's modulus of the bimorph, respectively.

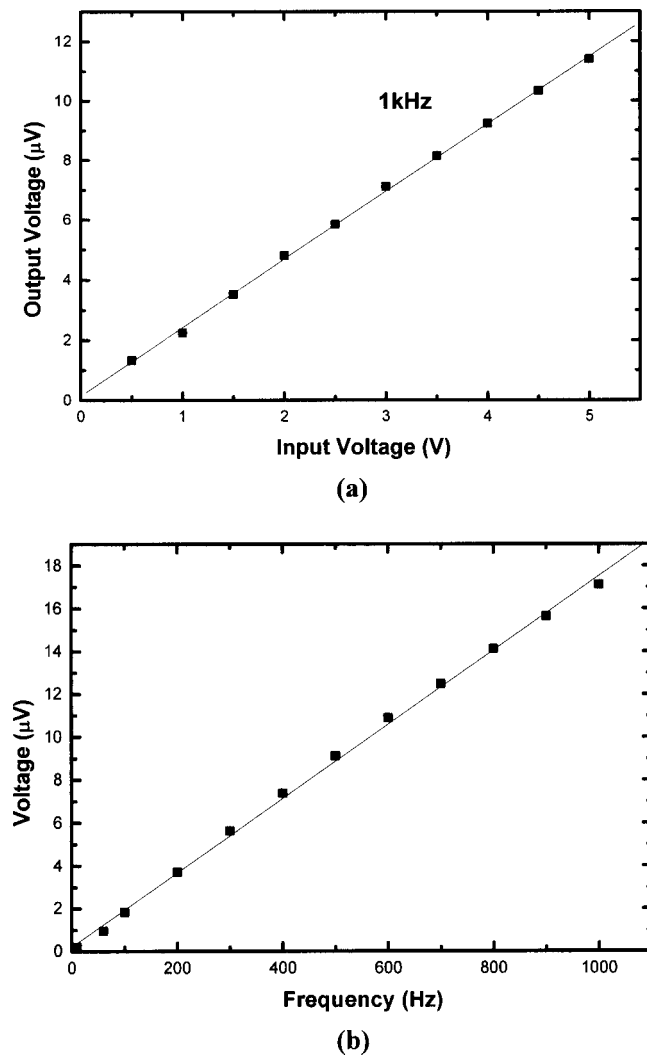


FIG. 6. (a) The output voltage of bimorph vs input voltage after using a low-noise current preamplifier SR570 in high-pass filter at 1 kHz, which also shows a good linear relationship. (b) The calibration when the signal is amplified by SR570. The sample is PMN/PT(65/35%) on platform in Fig. 4(a).

Equation (2) indicates that for a fixed displacement  $\Delta$  at point  $G$ , a shorter length of  $h$  and  $L$  in the sensor head will improve the sensitivity. The reason is that for a fixed displacement  $\Delta$ , a short length will result in a large force  $F$  in the bimorph [Eq. (1)], which results in a high charge output. However, for the strain measurement in soft polymer films, a large force at the sensor head will inevitably introduce a large error, which certainly imposed a limit on the lengths of  $h$  and  $L$  in the device.

In order to determine the optimum dimensions for the sensor length ( $h$  and  $L$ ), the possible error induced by the force at the sensor head (point  $G$ ) on soft polymer films in the strain measurement should be analyzed. From Newton's third law, it can be derived that this force should be equal to that produced in the sample due to the deformation ( $\Delta - \Delta_0$ ), i.e.,

$$F = A(\Delta - \Delta_0)Y^P/t_p, \quad (3)$$

where  $A$  is the contacting area of the probe head with the sample, which in our case is about  $A = \pi \times 0.35^2 \text{ mm}^2$ ,  $Y^P$  is

the Young's modulus and  $t_p$  is the thickness of the polymer, respectively.  $\Delta_0$  is the static displacement of the polymer when the force  $F$  was not imposed on the sample. Clearly, a small error due to the force at the sensor head requires  $\Delta_0/\Delta$  be nearly equal to one. Combining Eqs. (1) and (3) yields

$$\frac{\Delta}{B} = \frac{A(\Delta - \Delta_0)Y^P}{t_p}, \quad (4)$$

which, after the rearrangement, becomes

$$\frac{\Delta_0}{\Delta} = 1 - \frac{t_p}{ABY^P}.$$

To satisfy the condition that  $\Delta$  is nearly equal to  $\Delta_0$ , it is required that

$$\frac{AY^P}{t_p} \left[ \frac{4L^3}{3\pi Y^{\text{st}} r^4} + \frac{3h}{2wt^3 Y} (hL + L^2 + h^2/3) \right] \gg 1. \quad (5)$$

One interesting consequence of the inequality is that the error due to the force  $F$  at the sensor head is smaller in a thin film sample ( $t_p$  is small) compared with a thick one. Apparently, in order to reduce the error, a longer length of the bimorph and stainless steel pin ( $h$  and  $L$ ) is required, which was verified in our experiment.

If a sinusoidal field  $E = E_0 \sin \omega t$  is used to measure the strain of electrostrictive materials, it is the second harmonic component of the strain response that is measured by the lock-in amplifier

$$S = R(E_0 \sin \omega t)^2 = RE_0^2(1 - \cos 2\omega t)/2,$$

where  $R$  is the electrostrictive coefficient of copolymer and  $\omega$  is the angular frequency, respectively. From the above equation, one can get displacement of the polymer sample and then deduce the  $R$  from the calibration curve.

When operating at lower frequency, the frequency limit depends on the frequency range of the lock-in amplifier and the strain level of the copolymer sample. In this system, the limiting frequency of the SR850 lock-in amplifier is 0.005 Hz and the latter is caused by the increased noise of the environment and approximately proportional to  $1/f$  spectrum, where  $f$  is frequency.<sup>3</sup> At the high frequency end, the operation frequency is limited by the resonant frequency of the cantilever. For a cantilever beam, the resonant frequency is inversely proportional to the square of the length of stainless steel pin and bimorph [ $\sim 1/(h+L)^2$ ].<sup>9,10</sup>

#### IV. EXPERIMENTAL RESULTS

It is found that a slight change of current occurred when the sensor head contacts the sample as shown in Fig. 7. The output current decreased to a stable value after a few minutes. That may be caused by the leakage of charge because of the weak signal of the bimorph. But the current change will be eliminated by the SR570 in high-pass filter mode at low frequencies. It is also essential to make a fixed original point for every measurement and take an average value while using a long time constant of the lock-in amplifier.

Presented in Fig. 8(a) is the electric impedance versus frequency of No. 3 with one end clamped and the other free. It was measured by Agilent 4294A Precision Impedance

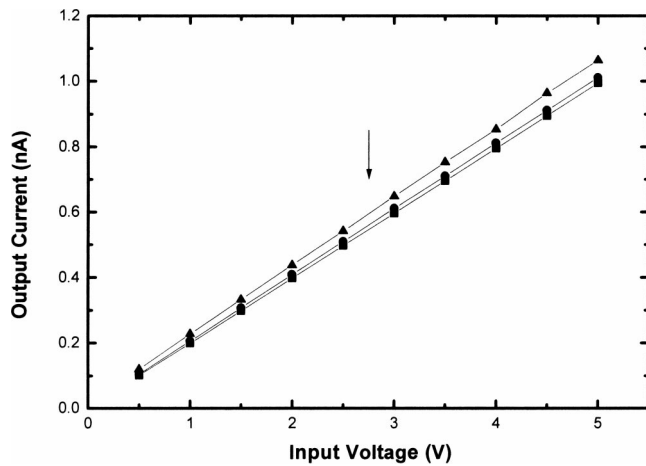
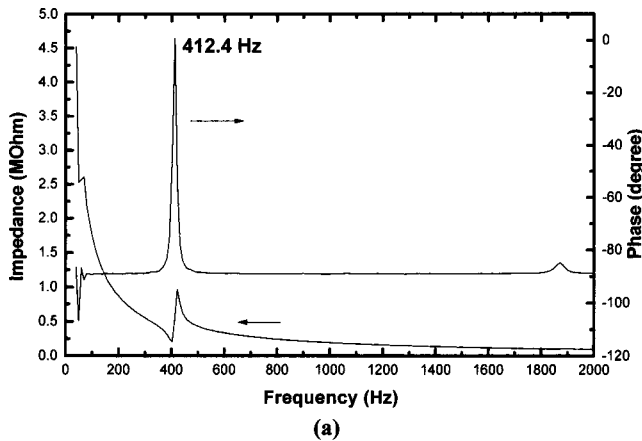
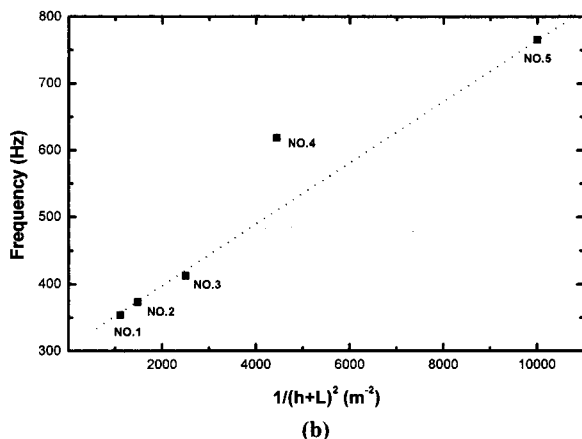


FIG. 7. The decrease of current to a stable value under a fixed position as time goes by which indicates a leakage of charge due to weak signal of the experiment setup. But it will be eliminated by SR570 in high-pass filter at low frequencies. The arrow indicates the trend of charge leakage.

Analyzer. A resonant frequency of 412.4 Hz was found below 2 kHz. Other sensor heads were also measured shown in Fig. 8(b). In Fig. 8(b), the resonant frequency without any load is raised by reducing the length of the stainless steel pin in agreement of theoretical prediction for a cantilever beam.



(a)



(b)

FIG. 8. (a) The electric impedance and phase of No. 3 sensor head as a cantilever beam with one end clamped and the other free. (b) The resonant frequencies of different sensor heads (square points) are inversely proportional to the square of the length of stainless steel pin and bimorph.

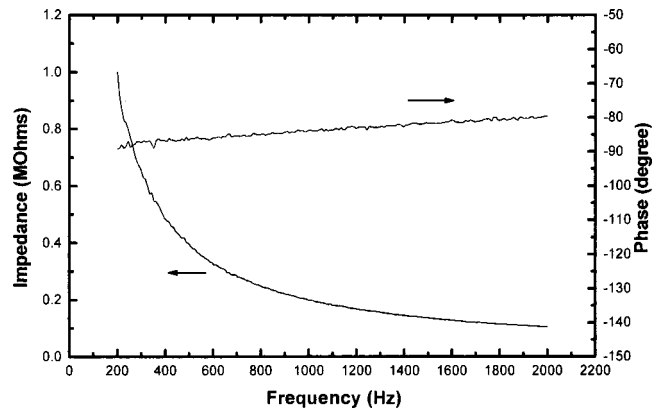


FIG. 9. The electric impedance and phase of No. 3 head measured from the bimorph when the probe head was in contact with a PZT sample on platform shown in Fig. 4(b). There is no resonance at frequencies below 2 kHz and the other sensor heads are similar to No. 3. When operating at low frequencies, a long time constant of a lock-in amplifier is preferred.

In order to get reliable measurements, it is important to operate below the resonant frequency.

Shown in Fig. 9 is the electric impedance versus frequency of the No. 3 head when the probe head was in contact with a PZT sample on platform shown in Fig. 4(b). It can be seen that there is no apparent resonance at frequencies below 2 kHz. One of the characteristics of the bimorph-based dilatometer is that it can be operated at very low frequency free from the resonance with reliability, so our setup can also work well at low frequency, for example, 10 Hz or 1 Hz.<sup>3</sup>

A commercial P(VDF-TrFE) (80/20 mol %) copolymer sample was used to calibrate the setup under low electric field. The sample was 16.5 mm × 19.5 mm in dimension with a thickness of 30  $\mu$ m and the  $d_{33}$  was about 25 pC/N. When a 10 V voltage was applied on it, the output voltage obtained from the sensor element was not stable at low frequencies as shown in Fig. 10. From the piezoelectric effect, the displacement caused by the electrical field in that copolymer film was very small at low frequencies, which leads to a weak output from the bimorph, so it is appropriate to choose a sample with a larger piezoelectric constant as calibration standard.

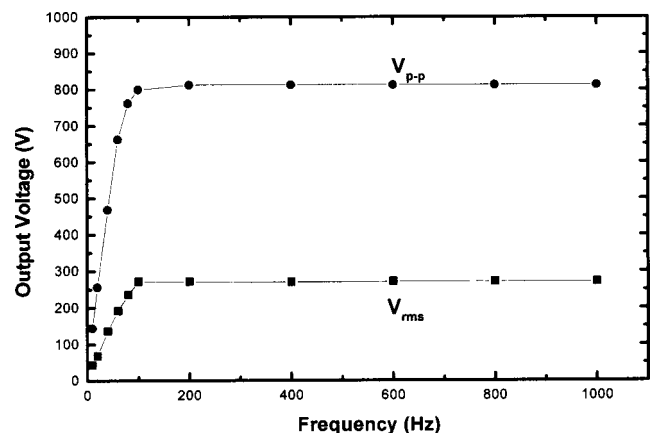


FIG. 10. The output voltage as a function of frequency when a commercial P(VDF-TrFE) (80/20 mol %, 25 pC/N, 30  $\mu$ m) copolymer film was used to calibrate the setup.  $V_{p-p}$  was the peak voltage and  $V_{rms}$  was the root of mean square voltage.

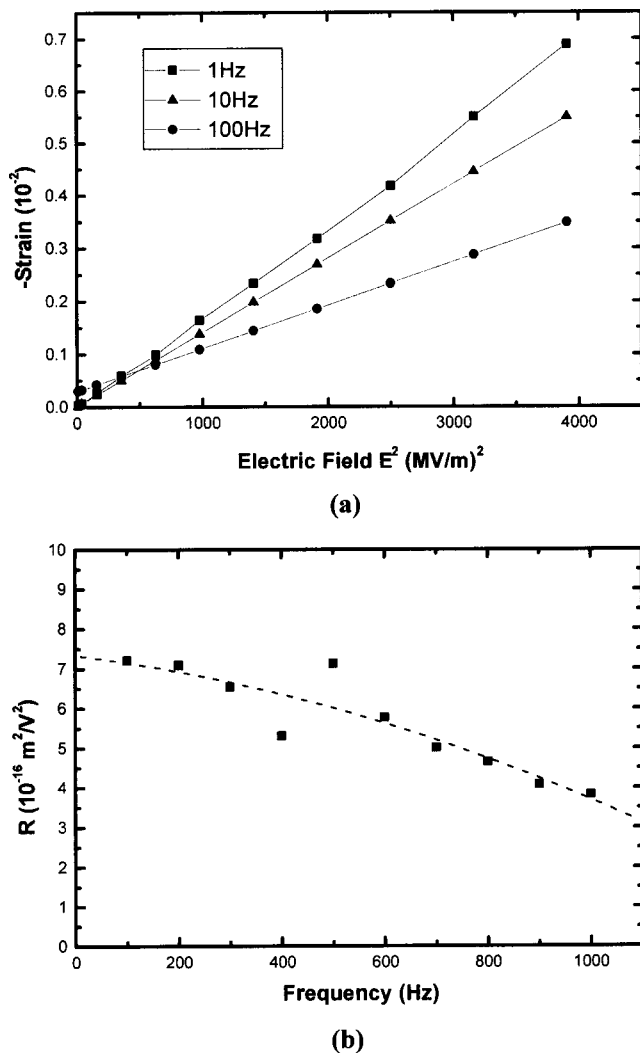


FIG. 11. (a) The amplitude of longitudinal strain as a function of the square of electric field for H<sup>+</sup> irradiated P(VDF-TrFE) (70/30 mol %, 107 Mrad) at 1 Hz, 10 Hz, and 100 Hz on platform in Fig. 4(b). (b)  $R$  coefficient of PMN/PT(65/35%) as a function of frequencies on platform in Fig. 4(a).

In polymeric materials, high-energy particle irradiation has been widely used to modify their properties, for example, phase transition, dielectric constant, etc.<sup>11</sup> For irradiated P(VDF-TrFE) copolymer films, it was found that very high longitudinal strain will be induced under high electric field while the transverse strain is relatively small.<sup>12</sup> A very high longitudinal electromechanical response in comparison with the transverse one can significantly enhance the influence of the lateral modes on the thickness resonance and improve the performance of the devices utilizing the longitudinal strain such as ultrasonic transducers, actuators and, sensors.<sup>13,14</sup> So it is a good way to evaluate the strain response of those copolymers at high electric field by the bimorph-based dilatometer.

Then we measured the electrostrictive coefficient  $R$  of some materials at room temperature. Figure 11(a) is a strain versus the square of electric field at different low frequencies of H<sup>+</sup> irradiated P(VDF-TrFE) (70/30 mol %, 107 Mrad) on platform shown in Fig. 4(b). It shows a good linear relationship between strain and the square of electric field. Because the irradiated copolymers will show typical features of the

relaxor ferroelectric, including dielectric constant peak broadened markedly, the electrostrictive coefficient  $R$  strongly depends on frequency.<sup>15,16</sup> According to early study, the electrostrictive coefficient  $R$  of P(VDF-TrFE) copolymers in the ferroelectric phase was extrapolated from the strain versus polarization hysteresis loop and found to be in the range from  $-3.19 \times 10^{-18} \text{ m}^2/\text{V}^2$  to  $-3.8 \times 10^{-18} \text{ m}^2/\text{V}^2$ .<sup>17</sup> But in a recent study for electron irradiated copolymers, the  $R$  was in the range from  $-0.6 \times 10^{-18}$  to  $-2.2 \times 10^{-18} \text{ m}^2/\text{V}^2$  at low frequency.<sup>18,19</sup> In Fig. 11(a), the  $|R|$  will slightly increase ( $R_{10 \text{ Hz}} = -1.408 \times 10^{-18} \text{ m}^2/\text{V}^2$ ) as the frequency decreases ( $R_{1 \text{ Hz}} = -1.718 \times 10^{-18} \text{ m}^2/\text{V}^2$ ) below 100 Hz.

Figure 11(b) is the electrostrictive coefficient  $R$  of PMN/PT(65/35%) using the platform shown in Fig. 4(a). As widely used electrostrictive materials, the frequency and temperature are the most important factors affecting the performance of  $R$  coefficient for PMN/PT relaxor ferroelectric.<sup>20,21</sup> In Fig. 11(b), the  $R$  was also increased ( $R_{1 \text{ kHz}} = 3.83 \times 10^{-16} \text{ m}^2/\text{V}^2$ ) as the frequency decreased ( $R_{100 \text{ Hz}} = 7.21 \times 10^{-16} \text{ m}^2/\text{V}^2$ ). But  $R$  became unreliable near resonance frequency (412.4 Hz) as shown at 400 Hz ( $R_{400 \text{ Hz}} = 5.31 \times 10^{-16} \text{ m}^2/\text{V}^2$ ). The appearance of the frequency dispersion in Figs. 11(a) and 11(b) is characteristic of the relaxor ferroelectric materials.<sup>22</sup>

Apparently, the results from the above discussion indicate that the device can be used reliably for the strain measurement in polymeric films and ceramics without imposing large stress or mechanical constrains, which implies the similar principle as other equipment.<sup>23,24</sup> It is believed that the bimorph-based dilatometer is an effective way in strain measurement with high sensitivity and stability.

## ACKNOWLEDGMENTS

This work was supported by the Centre for Smart Materials of The Hong Kong Polytechnic University. It was also supported in part by the National Natural Science Foundation of China under Grant Nos. 59973015 and 59943001.

<sup>1</sup>Q. M. Zhang, V. Bharti, and X. Zhao, *Science* **280**, 2101 (1998).

<sup>2</sup>X.-Z. Zhao, V. Bharti, and Q. M. Zhang, *Appl. Phys. Lett.* **73**, 2054 (1998).

<sup>3</sup>J. Su, P. Moses, and Q. M. Zhang, *Rev. Sci. Instrum.* **69**, 2480 (1998).

<sup>4</sup>Z.-Y. Cheng et al., *J. Appl. Phys.* **86**, 2208 (1999).

<sup>5</sup>M. Zhenyi, J. I. Scheinbeim, J. W. Lee, and B. A. Newman, *J. Polym. Sci., Part B: Polym. Phys.* **32**, 2721 (1994).

<sup>6</sup>R. F. Saraf, H. Tong, T. W. Poon, B. D. Silverman, P. S. Ho, and A. R. Rossi, *J. Appl. Polym. Sci.* **46**, 1329 (1992).

<sup>7</sup>H. Wang, Q. M. Zhang, L. E. Cross, R. Ting, C. Coughlin, and K. Rittenmyer, *Proceedings of the 9th IEEE International Symposium on Applications of Ferroelectrics*, 1994, p. 182.

<sup>8</sup>P. A. Lewin, M. E. Schafer, and R. C. Chivers, *Ultrasound Med. Biol.* **13**, 141 (1987).

<sup>9</sup>Landau and E. M. Lifshitz, *Theory of Elasticity* (Pergamon, Oxford, 1986).

<sup>10</sup>J. M. Herbert, *Ferroelectric Transducer and Sensors* (Gordon and Breach, New York, 1982).

<sup>11</sup>A. Lovinger, *Macromolecules* **18**, 190 (1985).

<sup>12</sup>Q. M. Zhang, Z.-Y. Cheng, V. Bharti, T.-B. Xu, H. Xue, T. Mai, and S. J. Gross, *Proc. SPIE* **3987**, 37 (2000).

<sup>13</sup>L. F. Brown, *IEEE Trans. Ultrason. Ferroelectr. Freq. Control* **47**, 1377 (2000).

- <sup>14</sup>H. Ohgashi, K. Koga, M. Suzuki, T. Nakanishi, and K. Kimura, *Ferroelectrics* **60**, 263 (1984).
- <sup>15</sup>A. Odajima, Y. Takasa, T. Ishibashi, and Y. Yuasa, *Jpn. J. Appl. Phys., Part 1* **24**, 881 (1985).
- <sup>16</sup>Y. Tang, X.-Z. Zhao, H. L. W. Chan, and C. L. Choy, *Appl. Phys. Lett.* **77**, 1713 (2000).
- <sup>17</sup>T. Furukawa and N. Seo, *Jpn. J. Appl. Phys., Part 1* **29**, 675 (1990).
- <sup>18</sup>Z.-Y. Cheng, V. Bharti, T.-B. Xu, Haisheng Xu, T. Mai, and Q. M. Zhang, *Sens. Actuators A* **90**, 138 (2001).
- <sup>19</sup>J. Su, Q. M. Zhang, and R. Ting, *Appl. Phys. Lett.* **71**, 386 (1997).
- <sup>20</sup>V. A. Isupov and E. P. Smirnova, *Ferroelectrics* **90**, 141 (1989).
- <sup>21</sup>L. J. Lin and T. B. Wu, *J. Am. Ceram. Soc.* **73**, 1253 (1990).
- <sup>22</sup>L. E. Cross, *Ferroelectrics* **76**, 241 (1987).
- <sup>23</sup>G. L. Miller, J. E. Griffith, E. R. Wagner, and D. A. Grigg, *Rev. Sci. Instrum.* **62**, 705 (1991).
- <sup>24</sup>T. Itoh and T. Suga, *J. Vac. Sci. Technol. B* **12**, 1581 (1994).